NMR Study of Kaolinite Intercalation Compounds with Formamide and Its Derivatives. 2. Dynamics of Guest Molecules

Xiulan Xie and Shigenobu Hayashi*

National Institute of Materials and Chemical Research, 1-1 Higashi, Tsukuba, Ibaraki 305-8565, Japan

Received: January 20, 1999; In Final Form: April 19, 1999

Dynamics of guest molecules in kaolinite intercalation compounds with formamide (FA), formamide-*N*,*N*-d_2 (FA-d_2), *N*-methylformamide (NMF), and *N*,*N*-dimethylformamide (DMF) has been investigated through ^{2}H NMR spectra and ^{2}H and ^{13}C spin−lattice relaxations. ^{2}H NMR spectra of kaolinite/FA-d_2 in the temperature range 200−350 K are composed of a narrow central peak, a resolved Pake doublet (RD_1), and a distribution of Pake doublets (RDs). Quadrupole coupling constants and asymmetric factors obtained by fitting the spectral patterns indicate that RD_1 is ascribed to the host hydroxyl group formed through H−D exchange during the synthesis and RDs to the guest molecules in the interlayer. Temperature dependence of the quadrupole coupling constant reveals that the guest molecules undergo librational motions and that the librational amplitude increases with temperature. Spin−lattice relaxations of ^{1}H and ^{29}Si spins are due to paramagnetic impurities. ^{29}Si spins relax through direct dipole−dipole interaction with electron spins, and spin diffusion plays a role in the ^{1}H relaxation. Variable-temperature ^{13}C spin−lattice relaxation times T_1 of kaolinite intercalates with FA, FA-d_2, NMF, and DMF were recorded at two magnetic fields. T_1 decreases with increasing temperature in all the samples and increases at the higher magnetic field in the order of FA > FA-d_2 > NMF > DMF, where it is almost independent of the field in kaolinite/DMF. ^{13}C spins relax through dipole−dipole interactions with ^{1}H and ^{14}N by the librational motions of the molecules. The field dependence indicates that the correlation times are of the order of nano-seconds, and that they are in the order of FA > FA-d_2 > NMF > DMF. The temperature dependence of the relaxation time is caused by the amplitude change of the librational motions. ^{2}H spins relax mainly through paramagnetic impurities being assisted by spin diffusion at low temperatures, and fluctuation of quadrupole interaction caused by the librational motions contributes to the relaxation at higher temperatures.

I. Introduction

Structures of kaolinite intercalation compounds have attracted great interest.[1−6] Crystal structures obtained by diffraction techniques are usually treated as first-hand data. However, when no such data are available, NMR serves as a powerful tool for providing information on local structures. There are no crystal structure data of kaolinite intercalation compounds with formamides. Analogy with those of the corresponding intercalates of dickite,[4] a two-layer monoclinic modification of kaolinite, is supposed to shed light on the structure of the kaolinite intercalates. Structure data of dickite/formamide (FA)[5] and dickite/*N*-methylformamide (NMF)[6] reveal an ordered layout of the guest molecules in the interlayer space with formation of 3-fold hydrogen bonds between the formamide oxygen and the hydroxyl groups of the adjacent aluminum hydroxide sheet in the samples: one hydrogen bond between the amide N and one of these hydroxyls, another between the amide NH and an oxygen of the adjacent silica sheet in kaolinite/FA, and no hydrogen-bond link between the amide group and the adjacent silica sheet in kaolinite/NMF. In our previous study,[7] we have investigated local structures and orientations of the guest molecules in kaolinite/FA, kaolinite/formamide-*N*,*N*-d_2 (FA-d_2), kaolinite/NMF, and kaolinite/*N*,*N*-dimethylformamide (DMF) mainly through ^{1}H, ^{13}C, and ^{29}Si NMR spectra: Guest molecules are regularly arranged in the interlayer space with a molecular guest/host ratio of 1.0, i.e., one guest molecule per each $Al_2Si_2O_5(OH)_4$ unit; ^{13}C and ^{1}H NMR spectra indicate that hydrogen bonds are formed between the guest molecules and the host layers, that the guest/host interaction is in the order FA > NMF > DMF, and that the mobility of the guest molecules is in the inverse order.

NMR has its advantage of being capable of providing dynamics information. Hayashi[8,9] has applied solid-state NMR to study dynamics of dimethyl sulfoxide (DMSO) molecules in kaolinite/DMSO intercalation compounds.

In the present work, we have investigated dynamics of the guest molecules in kaolinite intercalation compounds with FA, FA-d_2, NMF, and DMF mainly through ^{2}H and ^{13}C NMR. Spin−lattice relaxation times T_1 and spectra were measured under variable temperature conditions. The obtained results demonstrate that the interlayer guest molecules undergo librational motions. ^{29}Si and ^{1}H relaxation studies are also presented.

II. Experimental Section

The kaolinite used was Georgia kaolinite KGa-1 with a content of paramagnetic impurities of about 0.46 wt %, which is referred to as sample I. Kaolinite intercalation compounds were the same as those in our previous work[7] and thus the same notations were used; i.e., kaolinite/FA obtained by the displacement method, kaolinite/FA-d_2 by the vaporizing method, kaolinite/NMF by the vaporizing method, and kaolinite/DMF by the displacement method are referred to as samples II, III, IV, and V, respectively.

The NMR measurements were carried out by Bruker MSL400, ASX400, and ASX200 spectrometers with static magnetic field

10.1021/jp990238d CCC: $18.00
Published on Web 07/07/1999

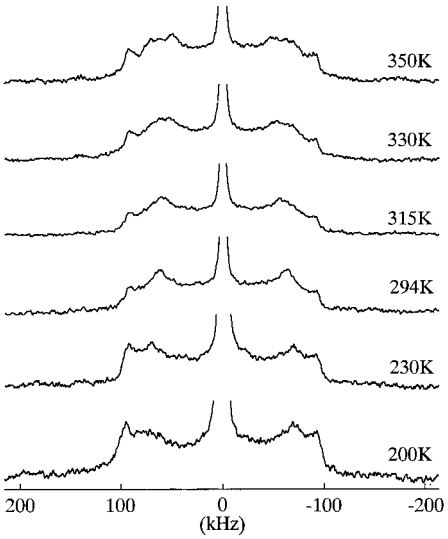

Figure 1. ^{2}H NMR spectra of kaolinite/FA-d_2 (sample III) measured at $\nu_L = 61.42$ MHz. Quadrupole echo pulse sequence was used with a pulse interval of 15 μs.

strengths of 9.4, 9.4, and 4.7 T, respectively. MSL400 was used for the measurements of ^{2}H static spectra (Larmor frequency of 61.42 MHz) and ^{1}H magic-angle-spinning (MAS) spectra (400.14 MHz), ASX400 for MAS spectra of ^{13}C (100.61 MHz) and ^{29}Si (79.50 MHz), and ASX200 for ^{13}C MAS spectra (50.32 MHz). ^{2}H spectra were recorded for static samples using a probehead with a solenoid coil, where the latter half of the echo signal was obtained with the quadrupole echo pulse sequence. ^{2}H T_1 was measured with the saturation recovery method in which the magnetization was first saturated by a string of near 90° pulses and then its recovery with time was monitored, being combined with the quadrupole echo pulse sequence for signal detection. ^{13}C and ^{29}Si T_1 was measured with Torchia's method,[10] and ^{1}H T_1 with the inversion recovery method, with all the measurements being carried out under MAS conditions. Spectra were presented with the following signals being 0 ppm or 0 Hz: neat tetramethylsilane for ^{13}C, ^{29}Si, and ^{1}H and D_2O for ^{2}H. The higher frequency side of the spectra with respect to the standard signal was expressed as positive. ^{2}H spectra were deconvoluted by Bruker WinFit version 1996 program.

FT-IR spectra were recorded at room temperature under N_2 gas flow by a Nicolet Avatar 360 spectrometer equipped with an attachment of diffuse reflectance measurements.

III. Results and Discussion

^{2}H NMR Spectra. Line shapes of ^{2}H NMR spectra reveal motions in the molecules. ^{2}H NMR spectra of kaolinite/FA-d_2 were recorded in the temperature range 200−350 K, as shown in Figure 1. The pattern is comprised of a narrow central (NC) peak, a resolved doublet (RD_1), and a distribution of Pake doublets (RDs). Although the resolved doublet indicates a rigid state of the guest molecules, a distribution of Pake doublets already shows that amount of molecules experience some kind of motions.

The signal intensity obtained by integrating over the whole spectra has a temperature dependence obeying Boltzmann distribution, which suggests absence of motions of the order of 100 kHz. We have also measured dependence of the line shape on the time interval between the two pulses in the quadrupole echo pulse sequence by changing the pulse interval from 5 to 300 μs in the temperature range of 200−350 K, and no dependence was observed. Therefore, motions with time constants of the order of 100 μs (10 kHz) are absent in the temperature range studied.

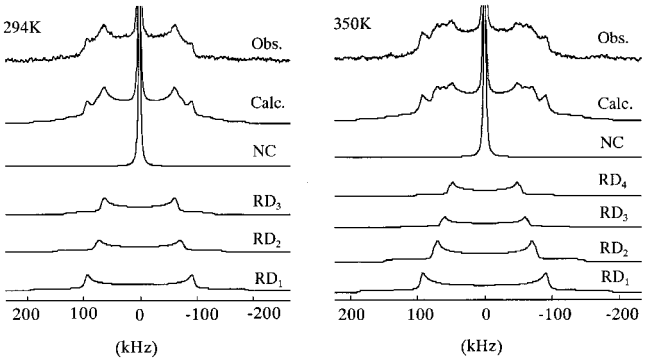

Figure 2. Deconvolution results of ^{2}H NMR spectra of kaolinite/FA-d_2 (sample III) measured at $\nu_L = 61.42$ MHz and at 294 and 350 K.

The spectra are deconvoluted into several components. Lorentzian line shape is assumed for the NC peak, and quadrupole coupling constants (e^2Qq/h), asymmetric factors (η_Q), and broadening factors are adjusted for RD_1 and RDs. Although the distribution in RDs might be continuous, discrete components are assumed to fit it. Figure 2 shows the results for the spectra at 294 and 350 K. An intense NC peak and a resolved doublet RD_1 are obtained as expected; two resolved components are required to account for the distributed doublets RDs at 294K and those lower, whereas three components are necessary for higher temperatures. Deconvolution results for all temperatures are listed in Table 1. In the whole temperature range, the NC component remains and the resolved doublet RD_1 has an asymmetric factor η_Q of 0.0. In the spectra at 200 and 230 K the signal-to-noise ratio is too low to obtain deconvoluted results without any assumptions. Since the fraction of RD_1 is independent of temperature at and above 294 K, the fraction is assumed to be 30% at the low temperatures. After subtracting the NC and RD_1 components, the residual pattern is fitted by the distributed doublets RD_2 and RD_3.

Table 1 reveals that RD_1 has e^2Qq/h values of 259−248 kHz in the temperature range of 200−350 K, while for the distributed doublets RDs the weighted average values are from 232 to 174 kHz in the same temperature range. Deuterium NQR studies[11] reported that the e^2Qq/h values for amino groups in deuterated acetamide, thioacetamide, nicotinamide, and propionamide are in the range of 197−207 kHz at 295 K, and the value for deuterated formamide was estimated to be 196 kHz. Accordingly, RDs has e^2Qq/h values reasonable for the ND_2 group, whereas the value for RD_1 suggests contribution from groups other than amides. Our previous study on deuterated kaolinite[12] showed that the e^2Qq/h values of hydroxyl groups in kaolinite are from 273 to 255 kHz in the temperature range of 150−350 K. Therefore, the RD_1 component results from OD groups of the kaolinite host. During the synthesis, H−D exchange between the guest ND_2 and the surface OH groups of the host took place. Deconvolution shows that the RD_1 component has a constant ratio of 30 ± 2% at 294 K and higher temperatures, which implies that the H−D exchange rate is slow enough in the intercalates where the guest molecules are fixed and/or that the exchange reaction arrived at the equilibrium state.

IR spectra present a further piece of evidence for the H−D exchange. IR spectra were recorded for kaolinite (sample I), deuterated kaolinite used in our previous work,[12] kaolinite/FA (sample II), and kaolinite/FA-d_2 (sample III). Sample I has a broad band with a fine structure at about 3650 cm^{-1} and a sharp

TABLE 1: ^{2}H Spectral Results of Kaolinite/FA-d_2 (sample III) Measured at ν_L = 61.42 MHz

	NC	RD_1		RD_2[a]		RD_3[a]		RD_4[a]	
T (K)	fwhm (Hz)	QCC (kHz)	η_Q	QCC (kHz)	η_Q	QCC (kHz)	η_Q	QCC (kHz)	η_Q
350	2500 (22)[b]	248 (29)	0.0	197 (23)	0.05	167 (12)	0.05	137 (14)	0.06
330	2500 (20)	252 (31)	0.0	199 (21)	0.05	171 (18)	0.06	143 (9)	0.05
315	2500 (24)	252 (28)	0.0	203 (19)	0.06	172 (23)	0.06	156 (6)	0.05
294	2800 (23)	252 (30)	0.0	207 (20)	0.05	173 (27)	0.05		
230	3100 (23)	252 (30)	0.0	241 (26)	0.05	195 (21)	0.05		
200	8000 (25)	259 (30)	0.0	258 (23)	0.06	205 (22)	0.05		

[a] Resolved doublet components composing the distributed Pake doublets RDs. [b] Values in parentheses show percentages of the components.

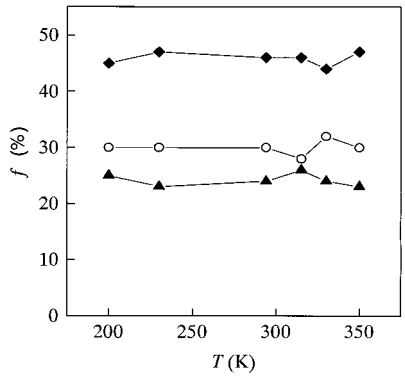

Figure 3. Temperature dependence of the fractions of NC (▲), RD_1 (○) and RDs (◆) in ^{2}H NMR spectra of kaolinite/FA-d_2 (sample III).

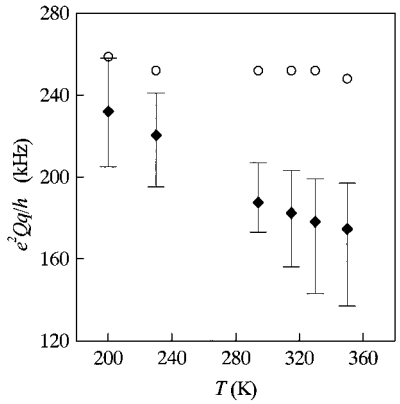

Figure 4. Temperature dependence of the quadrupole coupling constants of RD_1 (○) and RDs (◆) in kaolinite/FA-d_2 (sample III). The bars shows the distribution range.

peak at 3434 cm^{-1}, being ascribed to OH groups. The deuterated kaolinite has a new broad band centered at 2700 cm^{-1} also with a fine structure and a sharp peak at 2540 cm^{-1}, being assigned to OD groups, in addition to the band of the OH groups. In the range around 2700 cm^{-1}, sample II has bands at 2742 and 2667 cm^{-1}, being ascribed to FA molecules. Sample III has almost the same bands as the sample II does, except that a little bit stronger bands are observed at 2742 and 2677 cm^{-1} in the range around 2700 cm^{-1}. Detailed inspection reveals that sample III has very weak peaks at 2700 and 2540 cm^{-1} which are absent in sample II. Therefore, the IR results are consistent with the NMR results.

Temperature dependence of the fraction of each component is depicted in Figure 3. Fractions of RD_2, RD_3, and RD_4 were summed up to present that of the distributed doublets RDs. On the basis of the assumption of a constant ratio for RD_1, the three components show constant contributions throughout the temperature range within experimental errors. RD_1, which is due to the host O−D, has a contribution of 30 ± 2%; NC and RDs have contributions of 23 ± 3 and 47 ± 2%, respectively. NC is due to outersurface guest molecules, and the fraction of intercalation is estimated to be 0.67 (=47/(23 + 47)), assuming an equal H/D ratio in NC and RDs. In our previous studies,[7] ^{13}C NMR results revealed that the fraction of intercalated guest molecules was 57% in kaolinite/FA-d_2 at room temperature. ^{2}H and ^{13}C NMR results agree with each other within experimental errors.

Temperature dependence of e^2Qq/h is depicted in Figure 4. For the resolved doublet RD_1, its weak temperature dependence can be fitted into a linear regression: $e^2Qq/h = 266.1-0.05T$, where e^2Qq/h is in kHz and T stands for temperature in K. Our previous study on deuterated kaolinite[12] revealed the similar temperature dependence, where the regression was found to be $e^2Qq/h = 286.7-0.10\ T$. The two equations agree within experimental errors. Librational motions of the O−D groups, where D moves randomly on the bottom surface of a cone, was introduced to explain the e^2Qq/h temperature dependence and the asymmetry factor of 0.0. The diamonds with error bars in Figure 4 are weighted average e^2Qq/h values of RD_2, RD_3, and RD_4, which were assumed to present RDs in the simulation. The e^2Qq/h value of RDs obeys a linear regression: $e^2Qq/h = 312.8-0.41T$. Although motions with large amplitudes do not take place in the temperature range studied, librational motions with small amplitudes in the molecules result in the temperature dependence of the line shape. Distribution in the motional amplitude causes the distributed doublets pattern. Coefficient in the temperature dependence of e^2Qq/h reflects that the mobility of the guest molecules is larger than that of the host hydroxyl groups. The motion reduces the quadrupole coupling constant by a factor of $(3\cos^2\theta-1)/2$,[13] where θ is assumed to be an average librational angle. Supposing that the quadrupole coupling constants extrapolated to 0 K (266.1 and 312.8 kHz for the host hydroxyl group and the guest FA-d_2 molecules, respectively) correspond to values in their rigid states, the coupling constants at 350 K (248.0 and 172.5 kHz for the host hydroxyl group and the guest FA-d_2 molecules, respectively) produce θ of 12° and 33° for them, respectively. Using the similar assumptions, the librational amplitude was estimated to be 16° at 350 K for the hydroxyl group in deuterated kaolinite,[12] which agrees with the present results.

Quadrupole coupling constant is related to the strength of hydrogen bonding. Bulter et al.[14] has obtained an empirical relation between e^2Qq/h and the distance between two O atoms $R_{O\cdots O}$ in an O−H···O hydrogen bond from experimental data for various inorganic hydrate compounds. The relation is valid in the range of the quadrupole coupling constant of 57−240 kHz, which corresponds to $R_{O\cdots O}$ of 0.24−0.30 nm. Our previous study on deuterated kaolinite[12] showed that the e^2Qq/h value of 260 kHz at 293 K indicates the existence of relatively weak hydrogen bonds in kaolinite with the least $R_{O\cdots O}$ value of 0.30 nm. The e^2Qq/h value of RD_1 for the host O−D groups in kaolinite/FA-d_2 is 252 kHz at 294 K. Both values agree with each other within experimental errors and reveal weak hydrogen bonds in the samples.

An empirical correlation between $R_{O\cdots O}$ and the ^{1}H chemical shift in O−H···O hydrogen bonds has also been presented.[15] Our previous study[7] showed the chemical shift of 3.0 and 2.6 ppm for kaolinite and kaolinite/FA, respectively, which lead to $R_{O\cdots O}$ of 0.298 and 0.300 nm, respectively. Both the ^{1}H chemical shift and ^{2}H NMR results reveal that the hydroxyl groups in the host kaolinite structure is not much affected by intercalation.

The quadrupole coupling constant correlates also with the D···O distance in X−D···O hydrogen bonds (X = O, for the O−D group, and N, for the ND_2 group).[16,17] The empirical correlations obtained at 77 K are

$$\frac{e^2Qq}{h} = 310 - 0.572/R^3_{D\cdots O} \qquad \text{for} \qquad O-D\cdots O \qquad (1)$$

$$\frac{e^2Qq}{h} = 282 - 0.571/R^3_{D\cdots O} \qquad \text{for} \qquad N-D\cdots O \qquad (2)$$

where e^2Qq/h and $R_{D\cdots O}$ are in units of kHz and nanometers, respectively. For the host O−D group in kaolinite/FA-d_2, the observed e^2Qq/h value of 259 kHz at 200 K results in $R_{D\cdots O}$ of 0.224 nm. For the amide N−D, the weighted average e^2Qq/h value of 232 ± 26 kHz (200 K) produces $R_{D\cdots O}$ of 0.225 ± 0.063 nm. Deuterated kaolinite showed the e^2Qq/h value of 266 kHz (200 K),[12] which leads to an $R_{D\cdots O}$ value of 0.235 nm. These estimated values should be considered to be roughly approximated ones, since the empirical relations in eqs 1 and 2 were gained from considerably dispersed data at 77 K.

^{29}Si Relaxation. As reported in our previous studies on kaolinite of various origins[18] and kaolinite/DMSO intercalate,[8] ^{29}Si spins in those samples relax through interaction with electron spins on paramagnetic impurities. Under a MAS rate of 3.5 kHz spin diffusion between ^{29}Si spins is suppressed, and magnetization recovery recorded by Torchia's method can be described as[19]

$$M(t) = M_0 \exp[-(t/T_1)^{1/2}] \qquad (3)$$

where

$$\frac{1}{T_1} = \frac{16}{9}\pi^3 N_P^2 C \qquad (4)$$

$$C = \frac{2}{5}\gamma_I^2\gamma_e^2\hbar^2 S(S+1)\frac{\tau_e}{1+\omega_I^2\tau_e^2} \qquad (5)$$

where N_P is the concentration of the paramagnetic impurities, γ_I and γ_e are gyromagnetic ratios of I (^{29}Si) and electron spins, S is the spin quantum number of electron spins ($S = 1/2$), ω_I is Zeeman frequency of the I spin, and τ_e is the spin−lattice relaxation time of the electron spins.

Figure 5 shows semilogarithmic plots of the magnetization recovery curves as a function of square root of time. All the curves are linear, which means direct relaxation through the dipole−dipole interaction with electron spins on paramagnetic impurities.[18] The T_1 values deduced are listed in Table 2. The original kaolinite has the shortest T_1 of about 60 s, while the values for the single unresolved peaks corresponding to the intercalates in samples II, III, IV, and V are 91, 72, 92, and 121 s, respectively. The relaxation time increases upon expansion of the interlayer distance by intercalation. The relaxation time and the basal spacing d show the following relation: $T_1 = 21(\pm 15) + 63(\pm 14)d^2$ with T_1 in seconds and d in nanometers. The relation is consistent with the relaxation model applied where T_1 is in inverse proportion to N_p^2 as shown in eq 4. N_p is inversely proportional to the basal spacing.

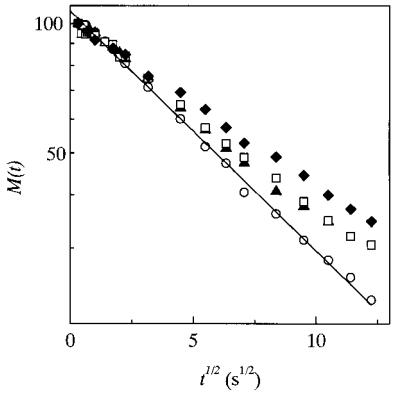

Figure 5. ^{29}Si spin−lattice relaxation curves of kaolinite (the −91.59 ppm peak in sample I) (○), kaolinite/FA (II) (▲), kaolinite/NMF (IV) (□), and kaolinite/DMF (V) (◆), measured at ν_L = 79.50 MHz, 298 K, and a spinning rate of 3.5 kHz with Torchia's method. The line is a least-squares fit for kaolinite.

TABLE 2: ^{29}Si (ν_L=79.49 MHz) and ^{1}H (400.14 MHz) Spin−Lattice Relaxation Times[a] of Kaolinite and Its Intercalates Measured under MAS

			^{29}Si		^{1}H		
no. of sample	guest	d^b (nm)	shift (ppm)	T_1 (s)	shift (ppm)	T_1(s)[c]	R^d
I		0.717	−90.97	56	2.0	0.08	17.0
			−91.59	62			
II	FA	1.019	−91.76	91	2.0	0.09	20.4
					8.0	0.07	36.0
III	FA-d_2	1.013	−91.75	72	2.0	0.08	25.0
					8.0	0.04	80.0
IV	NMF	1.080	−91.53	92	2.5	0.12	17.6
					6.7	0.13	19.5
					8.1	0.13	20.0
V	DMF	1.217	−92.42	121	2.9	0.12	10.0
					8.0	0.12	12.0

[a] Torchia's method with MAS of 3.5 kHz for ^{29}Si and inversion recovery method with MAS of 12.0 kHz for ^{1}H. The sample temperature was ambient: 298 K for ^{29}Si and 294 K for ^{1}H. [b] Basal spacing by X-ray powder diffraction.[7] [c] Weight-averaged ^{1}H relaxation time. [d] $R = T_{1l}/T_{1m}$.

Our previous study[8] on kaolinite intercalation with DMSO revealed that the dipole−dipole interaction between methyl protons in DMSO and ^{29}Si in the host contributes to the relaxation due to the CH_3 rotation. The kaolinite applied was of Kanpaku origin, and its ^{29}Si T_1 was 1500 s under MAS of 3 kHz. T_1 originated from the ^{1}H−^{29}Si dipole−dipole interaction in kaolinite/DMSO was estimated to be about 700 s. In the present study the contribution of the dipole−dipole interaction between the guest ^{1}H and the host ^{29}Si is masked even if it exists by the relaxation due to paramagnetic impurities whose concentration is higher than that in Kanpaku kaolinite.

^{1}H Relaxation. In kaolinite ^{1}H spins are relaxed by electrons spins on paramagnetic impurities.[18] However, the dipole−dipole interaction between protons is so large that spin diffusion plays a dominant role, and the relaxation is limited by the spin diffusion rate. The second moment of the dipole−dipole interaction between protons deduced from the crystal structure is 67 kHz^2.[20] MAS can affect the relaxation behavior through the effect on the spin diffusion rate in principle. However, the spinning effect was found to be small in kaolinite.[21] The spinning rate of about 10 kHz is not large enough to suppress the spin diffusion.

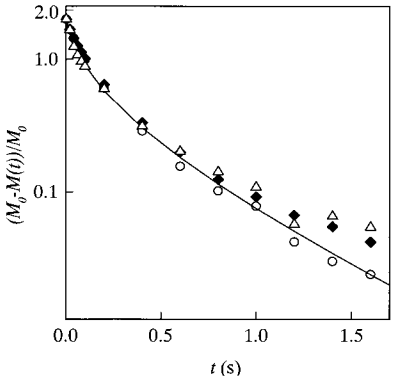

Figure 6. ^{1}H spin−lattice relaxation curves of kaolinite (sample I) (○) and kaolinite/FA (2.0 ppm (▲) and 8.0 ppm (△) in sample II), measured by the inversion recovery method at $\nu_L = 400.13$ MHz, 294 K, and a spinning rate of 12.0 kHz. The line is a fit to the kaolinite data.

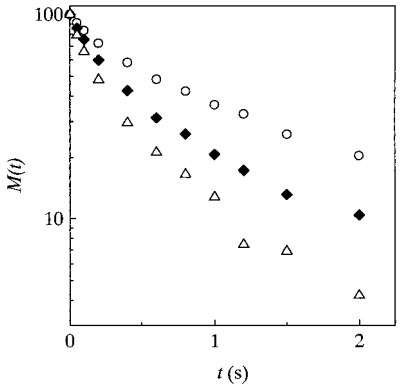

Figure 7. ^{13}C spin−lattice relaxation curves of kaolinite/FA (sample II), measured at 298 K (○), 315 K (◆), and 330 K (△) at $\nu_L = 100.61$ MHz and a spinning rate of 4.0 kHz with Torchia's method.

Figure 6 shows ^{1}H relaxation curves for the original kaolinite and kaolinite/FA (sample II) at a spinning rate of 12.0 kHz. The relaxation curves show nonexponential behavior. As studied in our previous work,[21] the nonexponentiality in kaolinite comes from the distribution of the relaxation time caused by inhomogeneous distribution of paramagnetic impurities. The best distribution function to fit the experimental data is that a population p is inversely proportional to the relaxation rate $1/T_1$.[21] T_1 is assumed to distribute from the longest value T_{1l} to the shortest value T_{1s}, with a middle point $T_{1m} = (T_{1l} + T_{1s})/2$. The calculated recovery curve for kaolinite is shown in Figure 6 as a solid line. The relaxation curves of the intercalates show behavior similar to those of the original kaolinite, and they are also analyzed using the same procedure.

Table 2 lists weight-averaged relaxation times T_{1av}. Protons of different origins within one sample relax similarly because of the fast spin diffusion. T_{1av} is 0.08 s for hydroxyl groups in the original kaolinite; 0.09 s for the kaolinite host and 0.07 s for HCO and NH_2 in sample II; 0.08 s for the host and 0.04 s for HCO and NH_2 in sample III; 0.12, 0.13 and 0.13 s for CH_3, NH and HCO in sample IV; and 0.12 s for both CH_3 and HCO in sample V. A distribution with $R = T_{1l}/T_{1m}$ around 20 is found for most of them, except $R = 80$ bound for sample III. The short T_{1av} (0.04 s) and the large R (80) for the carbonyl and amide protons in sample III is due to the large fraction of the outersurface guest molecules.

The T_1 values in Table 2 demonstrate that there is little contribution from motions of the guest molecules. In the case of the NMF and DMF intercalates, CH_3 rotation was expected to contribute to the ^{1}H relaxation through fluctuation of the dipole−dipole interaction between protons. However, the present results indicate that the CH_3 rotation is ineffective. A motion would contribute to the relaxation efficiently when the rate of the motion is of the order of Larmor frequency. Since the CH_3 rotation is hardly to stop, the ineffectiveness means that the rotation is too fast, i.e., much faster than 400 MHz.

In conclusion, ^{1}H spins in both the host kaolinite and the guest molecules are relaxed by paramagnetic impurities, and spin diffusion between protons plays a dominant role.

^{13}C Relaxation. The ^{13}C spin−lattice relaxation times T_1 were measured in the temperature range 298 to 330 K at two different magnetic fields with $\nu_L = 50.32$ and 100.61 MHz. Figure 7 shows magnetization recovery curves for sample II at different temperatures. There are nonexponentialities in the relaxation curves, which become more severe at higher temperatures. Since the spin diffusion between ^{13}C spins is neglected, relaxation caused by paramagnetic impurities can be described by eqs 3−5, which is the case for ^{29}Si. For kaolinite samples τ_e was estimated to be approximately several nanoseconds.[18] The relaxation time of ^{13}C through paramagnetic impurities is accordingly expected to be roughly the value for ^{29}Si, i.e., about 100 s. Therefore, relaxation mechanisms other than paramagnetic impurities should be taken into consideration. The temperature dependence suggests that the relaxation mechanism is of motional origins, and the nonexponentiality means a distribution of the relaxation time. The time in which the magnetization becomes $1/e$ of its initial value, T_{1est}, is accordingly chosen to be a representative value for T_1. The T_{1est} values obtained for the kaolinite intercalates are listed in Table 3.

In the temperature range studied T_{1est} decreases with increasing temperature for all the intercalates. T_{1est} increases with the magnetic field in kaolinite/FA (sample II), kaolinite/FA-d_2 (sample III), and kaolinite/NMF (sample IV), whereas it is almost independent of the field in kaolinite/DMF (sample V).

Inspection of the molecular structures of the guest molecules reveals that the possible relaxation mechanisms are (a) scalar coupling (SC) with ^{14}N, (b) dipole−dipole interaction with ^{14}N, and (c) dipole−dipole interaction with ^{1}H. For spins directly attached to quadrupolar nuclei, relaxation is found very often to be due to couplings with the quadrupolar nuclei because of the very quick quadrupolar relaxation.[22] Quantitative analysis of the mechanism (a) reveals that a minimum SC constant required for a relaxation time of the range of 1.0 s is about 4000 Hz, which is unreasonably large. In the mechanism (b) the estimated minimum relaxation time is 1.2 s. The T_{1est} values obtained at 294−330 K and 100.61 MHz are in the range of 0.28−2.97 s, and therefore mechanism (b) is not enough to explain the obtained relaxation time by itself. The mechanism (c) should work in addition to mechanism (b).

The ^{2}H NMR results in the FA-d_2 intercalate demonstrate that the guest molecules undergo librational motions with small amplitudes and no rotations of the whole molecule. ^{1}H relaxations in all the intercalates have no contribution from motions of the guest molecules. 180° flip of the NH_2 group in formamide is unlikely because of the double bond nature of the C−N bond. The hydrogen bond between the amide NH and O of the adjacent silica sheet in the FA intercalates also restricts the flip motion. For the NMF and DMF intercalates, the 180° flip of the amino group is neglected from the ^{13}C spectra. In kaolinite/DMSO,[8] ^{13}C relaxation is caused by methyl rotation around the C_3 axis, and T_1 at 294 K is 0.39 and 0.27 s for the keyed and unkeyed CH_3 groups, respectively. However, in kaolinite/NMF (sample IV) and kaolinite/DMF (sample V), T_1 of methyl groups at the same temperature is much longer: 2.97

TABLE 3: ^{13}C Spin−Lattice Relaxation Results of Kaolinite Intercalates Measured by Torchia's Method at ν_L = 100.61 MHz with a MAS Spinning Rate of 4.0 KHz

no. of sample	guest	shift[b] (ppm)	T_{1est}[a] (s) 298 K[c]	298 K	315 K	330 K
II	FA	168.6	0.65 ± 0.05	1.00 ± 0.05	0.48 ± 0.05	0.28 ± 0.05
III	FA-d_2	168.4	0.55 ± 0.05	0.80 ± 0.05	0.48 ± 0.05	0.38 ± 0.05
IV	NMF	164.2	1.31 ± 0.05	1.40 ± 0.10	0.91 ± 0.05	0.63 ± 0.05
		26.9	2.28 ± 0.12	2.97 ± 0.15	1.19 ± 0.05	0.73 ± 0.05
V	DMF	163.6	1.28 ± 0.05	1.20 ± 0.05	1.13 ± 0.05	0.66 ± 0.20
		38.8	1.12 ± 0.05	1.20 ± 0.05	1.11 ± 0.05	0.65 ± 0.25
		32.7	1.24 ± 0.05	1.43 ± 0.05	1.25 ± 0.05	0.29 ± 0.11

[a] Decay time in which the magnetization becomes 1/*e* of its initial value. [b] At 298 K. [c] Values measured at ν_L = 50.32 MHz.

± 0.15 s for NMF, and 1.20 ± 0.05 and 1.43 ± 0.05 s for the trans and cis positions in DMF, respectively. Rotation of the methyl groups in samples IV and V is considered to be too fast to be effective to the ^{13}C relaxation, as is the case in the ^{1}H relaxation. Moreover, the relaxation times of HCO are comparable to those of methyl groups. Librational motions of whole molecules, which was found to be the main cause in the temperature-dependent ^{2}H spectral pattern in kaolinite/FA-d_2, is the most reasonable to cause the relaxation in ^{13}C spins.

T_1 caused by dipole−dipole interaction with unlike spins can be expressed as follows:[23,24]

$$\frac{1}{T_1} = \frac{1}{3}S(S+1)\gamma_I^2\gamma_S^2\hbar^2\left(\frac{1}{r^6}\right)[J_0(\omega_I - \omega_S) + 3J_1(\omega_I) + 6J_2(\omega_I + \omega_S)] \quad (6)$$

where γ_I is a nuclear gyromagnetic ratio of ^{13}C spins, γ_S that of ^{1}H/^{14}N spins with spin S, and r the distance between ^{13}C and ^{1}H/^{14}N. $J_m(\omega)$, the spectral density at a frequency ω, is given by

$$J_m(\omega) = 2\int_0^\infty C_m(\Omega,t)\cos(\omega t)dt \quad (7)$$

and $C_m(\Omega,t)$ is the correlation function for the motion. Ω defines the dipole−dipole vector for dipole−dipole interaction, and orientation of the principal axes of the electric field gradient tensor for quadrupolar relaxation, with respect to the external magnetic field. Models for torsional dynamics, (a) an overdamped stochastic process and (b) reorientation described by Langevin equation for a damped harmonic oscillator, produce[25]

$$J_m(\omega) = \left(\frac{3}{2}\right)\langle\theta^2\rangle\frac{\tau_c}{1+\omega^2\tau_c^2} \quad (8)$$

where τ_c is the reorientational correlation time and $\langle\theta^2\rangle$ the angular excursion of the librational motion. $\langle\theta^2\rangle$ is dependent on temperature and can be expressed as

$$\langle\theta^2(T)\rangle = \langle\theta^2(0)\rangle T \quad (9)$$

Combining eqs 6 and 8, we obtain

$$\frac{1}{T_1} = \frac{S(S+1)\gamma_I^2\gamma_S^2\hbar^2}{2r^6}\langle\theta^2(T)\rangle\left[\frac{\tau_c}{1+(\omega_I-\omega_S)^2\tau_c^2} + \frac{3\tau_c}{1+\omega_I^2\tau_c^2} + \frac{6\tau_c}{1+(\omega_I+\omega_S)^2\tau_c^2}\right] \quad (10)$$

T_1 has its minimum value when τ_c is about the inverse of Larmor frequency. In the long-τ_c region, T_1 is proportional to the square of the static magnetic field. On the other hand, T_1 is independent of the field in the short-τ_c region.

The field dependence of T_{1est} in kaolinite/FA (sample II) reveals that the relaxation is on the long-τ_c region. For kaolinite/FA-d_2 (sample III), the field dependence of T_{1est} is weaker, still indicating the long-τ_c region of the relaxation, but closer to the minimum-T_1 point. For kaolinite/DMF, T_{1est} is field independent, and the relaxation is on the short-τ_c region; while a weak field dependence in kaolinite/NMF means a relaxation on the short-τ_c region near the minimum-T_1 point. At the minimum-T_1 point where $\omega_I\tau_c \cong 1$, τ_c is estimated to be on the order of nanoseconds. From the above discussion the τ_c values for the intercalates are in the order of FA > FA-d_2 > NMF > DMF, which agrees with the sequence of the strength in the guest−host interaction (FA > NMF > DMF) confirmed by our previous study mainly on ^{1}H and ^{13}C NMR spectra.[7] Kaolinite/FA-d_2 (sample III) has a shorter correlation time than kaolinite/FA (sample II), which might result from the weaker hydrogen bonds due to deuteration.

For the librational motions, the activation energy in τ_c is nearly zero, and the correlation time is almost independent of temperature. Temperature dependence of T_1 comes from that of the librational amplitude, which increases with increasing temperature as described by eq 9.

Several works have been reported for librational motions providing relaxation mechanisms. Williams et al.[26] have studied librational dynamics in a series of *N*-deuterated microcrystalline secondary amides mainly through ^{2}H spin−lattice relaxation time analysis: out-of-plane librations of the amide, which become overdamped due to both structural and conformation restraints, cause the spin−lattice relaxation. Other examples for relaxations due to small-angle librations were found in *n*-nonadecane-d_{40}/urea clathrate,[27] cyclopentane-d_{10},[28] bacteriorhodopsin,[29] and triose phosphate isomerase.[30]

^{2}H Relaxation. The ^{2}H T_1 values in kaolinite/FA-d_2 were measured in the temperature range between 200 and 330 K. The relaxation curves are plotted using the top point of the horns in RD_1 and the highest intensity position (assumed to be the average position) for RDs, although there might be a distribution of T_1 in the whole line shape.[31] Figure 8 shows the saturation recovery curves of RD_1 and RDs at 294 K.

The saturation recovery curves show nonexponentiality with a large distribution of the relaxation time. The time in which the value $(M_0 - M(t))/M_0$ becomes 1/*e* of its initial one T_{1est} is accordingly chosen to be a representative value for T_1. The T_{1est} values obtained are listed in Table 4. The accuracy ranges listed in the table were estimated from the scatter of the experimental data points.

The T_{1est} value decreases with increase in temperature, demonstrating contribution of molecular motions. At low temperatures where motions are greatly reduced paramagnetic impurities may contribute to the relaxation. The ^{29}Si spin−lattice relaxation time is 72 s, where the relaxation is caused by the direct dipole−dipole interaction with electron spins. The ^{1}H

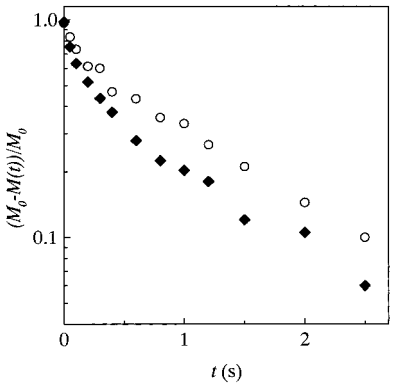

Figure 8. ^{2}H spin−lattice relaxation curves of RD_1 (○) and RDs (◆) in kaolinite/FA-d_2 (sample III) measured at 294 K and $\nu_L = 61.42$ MHz.

TABLE 4: ^{2}H Spin−Lattice Relaxation Time of Kaolinite/FA-d_2 (sample III)[a]

	T_{1est}[b] (s)	
T (K)	RD_1	RDs
200	1.41 ± 0.11	1.19 ± 0.19
294	0.84 ± 0.06	0.42 ± 0.05
315	1.00 ± 0.22	0.32 ± 0.05
330	0.72 ± 0.10	0.28 ± 0.05

[a] Measured by the saturation recovery method at $\nu_L = 61.42$ MHz. [b] Decay time in which the value $(M_0 - M(t))/M_0$ becomes $1/e$ of its initial one.

relaxation time is 0.08 s for the host hydroxyl groups, where the spin diffusion plays a role. The dipole−dipole interaction between ^{2}H spins is much smaller compared with that between ^{1}H spins, and consequently the spin diffusion rate is much lower. The estimated T_1 value of ^{2}H is 2.4 s in a completely deuterated sample, if the spin diffusion works effectively. At 200 K the obtained T_{1est} values are 1.41 ± 0.11 and 1.19 ± 0.19 s for the host O−D and the guest ND_2, respectively. The above estimation and the comparable T_1 values for the two groups suggest that paramagnetic impurities contribute to the relaxation considerably at 200 K. The relaxation time decreases monotonically with increasing temperature. At temperatures higher than 200 K, ^{2}H spins relax through fluctuation of the quadrupole interaction caused by the librational motions. The librational amplitude increases with temperature. The RDs component shows temperature dependence larger than the RD_1 component. This fact indicates that the guest molecules have larger librational amplitudes than the host hydroxyl groups, which is in agreement with the ^{2}H NMR spectral results.

IV. Conclusions

Dynamics of guest molecules has been studied by means of ^{2}H NMR spectra and ^{29}Si, ^{1}H, ^{13}C, and ^{2}H spin−lattice relaxations in kaolinite and its intercalation compounds with FA, FA-d_2, NMF, and DMF and the following conclusions have been made. (1) ^{2}H spectra of kaolinite/FA-d_2 in the temperature range of 200−350 K comprise a NC component, a resolved Pake doublet RD_1, and a distribution of Pake doublets RDs. The NC component is ascribed to outer surface guest molecules. RD_1 is the host OD formed through the H−D exchange during the synthesis, and RDs the guest molecules in the interlayer. Temperature dependence of the ^{2}H quadrupole coupling constant reveals librational motions of the host hydroxyl groups and the interlayer guest molecules. The librational amplitude increases with temperature, which is larger in the guest molecules than in the host hydroxyl groups. (2) ^{29}Si and ^{1}H spins are relaxed by paramagnetic impurities. ^{29}Si spins relax through direct dipole−dipole interaction with electron spins, while spin diffusion plays a dominant role in the ^{1}H relaxation. (3) ^{13}C spins relax through fluctuation of the dipole−dipole interaction with ^{1}H and ^{14}N caused by librational motions of the guest molecules with small amplitudes. Field dependence indicates that the correlation times are on the order of nanoseconds and that they are in the order of FA > FA-d_2 > NMF > DMF. Temperature dependence of the relaxation time is due to that in the librational amplitude. (4) In kaolinite/FA-d_2, paramagnetic impurities contribute to the ^{2}H relaxation considerably at lower temperatures. At temperatures higher than 200 K librational motions contribute to the relaxation through fluctuation of quadrupole interaction. ^{2}H T_1 decreases with temperature due to increase in the librational amplitude. The amplitude is larger in the guest molecules than in the host OD groups.

Acknowledgment. The authors are grateful to Prof. K. Kuroda of Waseda University for providing the original kaolinite sample. X.X. acknowledges the STA Fellowship given by the Science and Technology Agency of Japan.

References and Notes

(1) Adams, J. M.; Jefferson, D. A. *Acta Crystallogr*. **1976**, *B32*, 1180.
(2) Adams, J. M. *Clays Clay Miner*. **1978**, *26*, 291.
(3) Adams, J. M. *Acta Crystallogr*. **1978**, *B35*, 1084.
(4) Newnham, R. E. *Mineral Mag*. **1961**, *32*, 683.
(5) Adams, J. M.; Jefferson, D. A. *Acta Crystallogr*. **1976**, *B32*, 1180.
(6) Adams, J. M. *Acta Crystallogr*. **1979**, *B35*, 1084.
(7) Xie, X.; Hayashi, S. *J. Phys. Chem*. Submitted for publication.
(8) Hayashi, S. *J. Phys. Chem*. **1995**, *99*, 7120.
(9) Hayashi, S. *Clays Clay Miner*. **1997**, *45*, 724.
(10) Torchia, D. A. *J. Magn. Reson*. **1978**, *30*, 613.
(11) Loewenstein, A. *Advances in Nuclear Quadrupole Resonance*, **1983**, *5*, 53.
(12) Hayashi, S.; Akiba, E.; Miyawaki, R.; Tomura, S. *Clays Clay Miner*. **1994**, *42*, 561.
(13) Barnes, R. G. *Advances in Nuclear Quadrupole Resonance* **1974**, *1*, 335.
(14) Bulter, L. G.; Brown, T. L. *J. Am. Chem. Soc*. **1981**, *103*, 6541.
(15) Yesinowski, J. P.; Eckert, H. *J. Am. Chem. Soc*. **1987**, *109*, 6274.
(16) Hunt, M. J.; Mackay, A. L. *J. Magn. Reson*. **1974**, *15*, 402.
(17) Hunt, M. J., Mackay, A. L. *J. Magn. Reson*. **1976**, *22*, 295.
(18) Hayashi, S.; Ueda, T.; Hayamizu, K.; Akiba, E. *J. Phys. Chem*. **1992**, *96*, 10928.
(19) Abragam, A. *The Principles of Nuclear Magnetism*, 1st ed.; Oxford University Press: London, 1961; p 378.
(20) Hayashi, S.; Ueda, T.; Hayamizu, K.; Akiba, E. *J. Phys. Chem*. **1992**, *96*, 10922.
(21) Hayashi, S.; Akiba, E. *Solid State NMR* **1995**, *4*, 331.
(22) Hayashi, S.; Hayamizu, K.; Yamamoto, O. *J. Magn. Reson*. **1980**, *37*, 17.
(23) Torchia, D. A.; Szabo, A. *J. Magn. Reson*. **1982**, *49*, 107.
(24) Wittebort, R. J.; Szabo A. *J. Chem. Phys*. **1978**, *69*, 1722.
(25) Usha, M. G.; Peticolas, W. L.; Wittebort, R. J. *Biochemitry*, **1991**, *30*, 3955.
(26) Williams, J. C.; McDermott, A. E. *J. Phys. Chem. B* **1998**, *102*, 6248.
(27) Greenfield, M.; Vold, R. L.; Vold, R. R. *Mol. Phys*. **1989**, *66*, 269.
(28) Mack, J. W.; Torchia, D. A. *J. Phys. Chem*. **1991**, *95*, 4207.
(29) Kinsey, R. A.; Kintanar, A.; Oldfield, E. *J. Biol. Chem*. **1981**, *256*, 9028.
(30) Williams, J. C.; McDermott, A. E. *Biochemistry* **1995**, *34*, 8309.
(31) Hoatson, G. L.; Vold, R. L. *NMR Basic Princ. Prog*. **1994**, *32*, 1.